Numerical simulation of dual frequency etching reactors: Influence of the external process parameters on the plasma characteristics

V. Georgieva[a] and A. Bogaerts
Plasma, Laser Ablation and Surface Modeling ANTwerp (PLASMANT), Department of Chemistry, University of Antwerp, Campus Drie Eiken (CDE), Universiteitsplein 1, B-2610 Wilrijk-Antwerp, Belgium

(Received 1 February 2005; accepted 3 June 2005; published online 29 July 2005)

A one-dimensional particle-in-cell/Monte Carlo model is used to investigate $Ar/CF_4/N_2$ discharges sustained in capacitively coupled dual frequency reactors, with special emphasis on the influence of the reactor parameters such as applied voltage amplitudes and frequencies of the two voltage sources. The presented calculation results include plasma density, ion current, average sheath potential and width, electron and ion average energies and energy distributions, and ionization rates. The simulations were carried out for high frequencies (HFs) of 27, 40, 60, and 100 MHz and a low frequency (LF) of 1 or 2 MHz, varying the LF voltage and keeping the HF voltage constant and vice versa. It is observed that the decoupling of the two sources is possible by increasing the applied HF to very high values (above 60 MHz) and it is not defined by the frequency ratio. Both voltage sources have influence on the plasma characteristics at a HF of 27 MHz and to some extent at 40 MHz. At HFs of 60 and 100 MHz, the plasma density and ion flux are determined only by the HF voltage source. The ion energy increases and the ion energy distribution function (IEDF) becomes broader with HF or LF voltage amplitude, when the other voltage is kept constant. The IEDF is broader with the increase of HF or the decrease of LF. © *2005 American Institute of Physics*. [DOI: 10.1063/1.1989439]

I. INTRODUCTION

Glow discharges sustained by a radio-frequency source are widely used for material processing in the microelectronics. The dual frequency systems were introduced in the early 1990s (Refs. 1 and 2) but recently there has been an increasing interest and study of these systems.[3–12] The two-frequency scheme allows independent control of the ion flux and ion bombardment energy, which is important for surface etching applications, and this cannot be achieved by the conventional capacitively coupled (cc) reactor. In addition, it provides a significantly wider ion bombardment energy range in comparison with the one-frequency configuration.

Goto *et al.*[1] introduced the dual frequency setup and demonstrated its advantages in low ion energy etching. He proposed a high-frequency (HF), e.g., 13.56, and a very high-frequency (VHF), e.g. 100 MHz, scheme. Later on, low-frequency (LF), e.g., 2 MHz and below, and HF or VHF systems are employed.[2–12] Further numerical investigations showed that the plasma density was predominantly determined by the primary HF source while the self-bias and ion bombardment energy were determined by the secondary LF source.[2,3] The experimental study of Ar and Ar/CF_4 plasma structures in LF-HF reactors demonstrated that LF biasing and HF plasma production could be separated by increasing the sustaining frequency from 13.56 to 100 MHz.[4] However, if the source frequencies are close to each other (e.g., 6.78 and 13.56 MHz) the nonlinear interaction effects can be strong and the resulting plasma characteristics cannot be independently controlled.[5] In previous papers, we studied numerically the influence of the secondary frequency on the plasma characteristics and made a detailed investigation of the ion energy distribution function (IEDF) in $Ar/CF_4/N_2$ plasmas by means of the particle-in-cell/Monte Carlo (PIC/MC) method.[7,8] The PIC/MC method was employed also to study asymmetric dual frequency reactors[9–12] and to investigate the optimal reactor parameters for independent control of ion current and ion bombardment energy.[12]

Most of the numerical papers deal with Ar plasma because of its simple chemistry.[2,3,9–12] Plasma chemical issues are as much important in further optimization of etching processes as plasma processing units. Feedgas mixes are usually complex because of the conflicting requirements on the etch rate, selectivity to mask, and anisotropy. Carbon tetrafluoride, CF_4, is a basic component in gas mixtures for plasma etching of silicon and silicon dioxide, and therefore it is the most well-studied etch system (e.g., Refs. 1 and 13). While the investigation of pure CF_4 discharges gives the pattern for describing plasma etching, the study of discharges in CF_4 mixtures, which are often used for etching, provides insight into the process.[4–8,14]

This work presents the study of the complex gas mixture $Ar/CF_4/N_2$, used for etching in a dual frequency reactor at different applied frequencies and voltages of the two power sources by means of a PIC/MC method. Special attention is given to the conditions when the independent control of the ion flux and energy is possible because this is the main advantage of the two-frequency scheme. To our knowledge there are only computer simulations of the influence of the LF source in Ar discharges (e.g., Refs. 9–12). There are also investigations of complex gas mixtures, however, by hybrid or fluid model in magnetically enhanced cc single and dual frequency reactors (e.g., Refs. 15 and 16). The present

[a]Electronic mail: violeta.georgieva@ua.ac.be

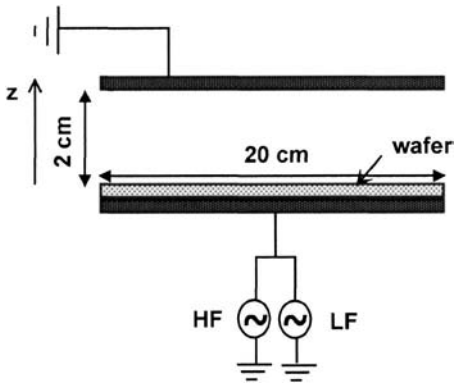

FIG. 1. Schematic diagram of the dual frequency reactor.

PIC/MC model is one dimensional because a two-dimensional PIC/MC for a complex gas mixture including electronegative gas is computationally time consuming, and it would not present physical trends, which are different from the one-dimensional model. However, we are currently working on a spherical one-dimensional PIC/MC to simulate asymmetric discharges. One set of simulations is carried out at a LF of 2 MHz and HFs of 27, 40, 60, and 100 MHz and keeping the HF or LF voltage amplitude constant, while the other voltage amplitude is varying. Another set of simulations is performed for (27+2) and (27+1) MHz at different values of constant HF voltage amplitude, while the LF voltage amplitude is varying. An additional set of simulations is carried out in a single frequency reactor at a HF of 60 MHz and varying the driving voltage amplitude in order to make a comparison with the dual frequency scheme.

In Sec. II the input parameters and the outline of the model are given. In Sec. III the results of the simulation, such as the plasma density, ion current, electron and ion average energies and energy distributions, average sheath potential and width, and ionization rates, are presented and discussed. Finally, in Sec. IV a summary is given. In order to facilitate the reader, who might be more familiar with the applied power than voltage, we present the calculated power of the two sources, corresponding to the applied voltages in the Appendix.

II. DESCRIPTION OF THE MODEL

A schematic diagram of the dual frequency cc reactor considered in this study is shown in Fig. 1. The plasma is sustained between two parallel plates, each 20 cm in diameter and separated from each other by 2 cm. One of the electrodes is driven by a dual frequency voltage source, i.e., the applied voltage is a sum of the HF and LF voltages

$$V = V_{\mathrm{HF}} \sin(\omega_{\mathrm{HF}} t) + V_{\mathrm{LF}} \sin(\omega_{\mathrm{LF}} t), \tag{1}$$

where V_{HF} and V_{LF} are the HF and LF voltage amplitudes, and ω_{HF} and ω_{LF} are the applied HF and LF. The other electrode is grounded. The computation is based on a one-dimensional coordinate space and three-dimensional velocity space PIC/MC algorithm. The motion of the charged particles is simulated by the PIC method using the standard explicit "leap frog" finite difference scheme.[17] The collisions between the charged particles are added by combining the PIC model with a MC procedure.[18,19] In the case of modeling of electronegative discharges, the major disadvantage of this method is the long computation time needed to reach convergence. The negative charges are confined in the bulk plasma and the only loss mechanism, i.e., ion-ion recombination, has a relatively low reaction frequency. Kawamura *et al.*[20] point out many physical and numerical methods of speeding up the PIC calculations. Some of these methods, such as longer ion time steps, different weights for electrons and ions, and improved initial density profiles, are also applied in the present simulation.

The charged species, which are followed in the model, are electrons, Ar^+, CF_3^+, N_2^+, F^-, and CF_3^- ions. The interactions between the particles are treated by a Monte Carlo method, which is basically a probabilistic approach. To calculate collision probabilities, it is necessary to have the corresponding collision cross-section data, which are not always available. Hence, the present model uses several techniques to define the collision probabilities even when the collision cross sections are unknown. The outlines of all techniques as well as all the data for electron-neutral (Ar, CF_4, and N_2) and ion-neutral collisions, electron-ion and ion-ion recombinations considered in the model are given in our previous papers.[7,8,14] The collisions of electrons with other neutrals, such as CF_4 radicals (CF_3, CF_2, CF, and F), excited states of N_2, and atomic nitrogen can significantly influence the ion and electron densities, and electron temperature, depending on the power, pressure, flow rate, etc. The present model does not take into account these collisions and the approximation is reasonable based on the following considerations. The computational and experimental results in a pure CF_4 discharge show that the densities of the radicals at low pressure are much lower in comparison with the CF_4 density, with values in the order of 10^{18} m^{-3}.[21,22] An experimental investigation of dc magnetron Ar/N_2 discharges at a pressure of 25 mTorr demonstrates that the atomic nitrogen equals between 0.13% and 0.24% of the molecular nitrogen depending on the fractional N_2 concentration.[23] Consequently, in the investigated gas mixture, which consists of 80% Ar, 10% CF_4, and 10% N_2, and at low pressure (30 mTorr) the concentration and the collision frequency of the other neutrals with the electrons are expected to be much smaller than the concentration and the collision frequency of the background gas neutrals with the electrons. In addition, in comparison with the PIC/MC method, a fluid or hybrid model[14,15] is more suitable to follow the radicals and excited states, since the PIC/MC method assumes that the background gas neutrals are distributed uniformly in the discharge, which is not applicable to the other neutral species (e.g., see the space distributions of CF and CF_2 presented in Ref. 22). On the other hand, the PIC/MC is more suitable to present the discharge dynamics and detailed behavior of the electron and ion energies, as is focused on in the present work.

We recall here only the expression for the energy width ΔE, centered at $e\bar{V}_s$, of the IEDF in dual frequency reactors, which was obtained in Ref. 8 and will be used in Sec. III to discuss the results.

$$\Delta E = \frac{8\lambda_2 e\bar{V}_s}{3\bar{s}\omega_{\mathrm{LF}}}\left(\frac{2e\bar{V}_s}{M}\right)^{1/2}, \tag{2}$$

where $\bar{V}_s$ and $\bar{s}$ are the average sheath potential and width, respectively, λ_2 is a parameter determined from the sheath potential plot as a function of the phase in the LF cycle and $\lambda_2 \leqslant 1$, ω_{LF} is the applied LF, M is the mass of the ion, and e is the electron charge.

The average electron and ion energies $\langle \varepsilon_{e,i} \rangle$ presented below are obtained from the electron energy distribution function (EEDF) and the IEDF, respectively, denoted as $F_{e,i}(\varepsilon)$,

$$\langle \varepsilon_{e,i} \rangle = \frac{\int_0^\infty \varepsilon_{e,i} F(\varepsilon_{e,i}) d\varepsilon}{\int_0^\infty F(\varepsilon_{e,i}) d\varepsilon}. \tag{3}$$

III. RESULTS AND DISCUSSION

The calculations are performed for an $Ar/CF_4/N_2$ mixture at a ratio of 0.8/0.1/0.1. All simulations are carried out at a pressure of 30 mTorr. The gas temperature is set to 300 K. The simulation grid is uniform and it consists of 100 cells. The electron time step varies from 10^{-11} to 3.7×10^{-11} s depending on the electron plasma frequency. To speed up the calculation, the ion time step is set to be 25 times longer than the electron time step, and different weights for electrons and ions are applied. The choice of the grid spacing and the time steps is defined by the accuracy criteria for the PIC/MC codes with explicit mover.[20] The typical results of this model are the electron and ion densities, fluxes and energy distributions, collision rates, and electric-field and potential distributions.

A. From HF to VHF, keeping the HF voltage amplitude constant and varying the LF voltage amplitude

Figure 2 presents the simulation results, averaged over one or two LF cycles, for the plasma density in the discharge center (a), the ion current density at the powered electrode (b), the electron energy in the discharge center (c), and the sheath potential (d) and width (e), as a function of the LF voltage amplitude. The calculated characteristics for the (27+2)-MHz case are averaged over two LF cycles since one LF cycle does not contain an integer number of HF cycles. The operating conditions are the following: the HF is chosen to be 27, 40, 60, or 100 MHz and the LF is 2 MHz; the HF voltage amplitude is kept at 200 V and the LF voltage amplitude is 0, 100, 200, 300, or 400 V. It can be seen that for all investigated frequency schemes the introduction of the second LF voltage source decreases the plasma density in the discharge center [Fig. 2(a)]. Further, the drop is not very pronounced for the (60+2)- and (100+2)-MHz cases, while it decreases more clearly with increasing LF voltage for the other two-frequency schemes, i.e., (27+2) and (40 +2) MHz. This means that for the latter cases the applied LF has influence on the plasma density as well as on the ion current density and electron energy, as it is observed below [Figs. 2(b) and 2(c)], and decoupling is impossible to be achieved. A drop of the plasma density with increase of the

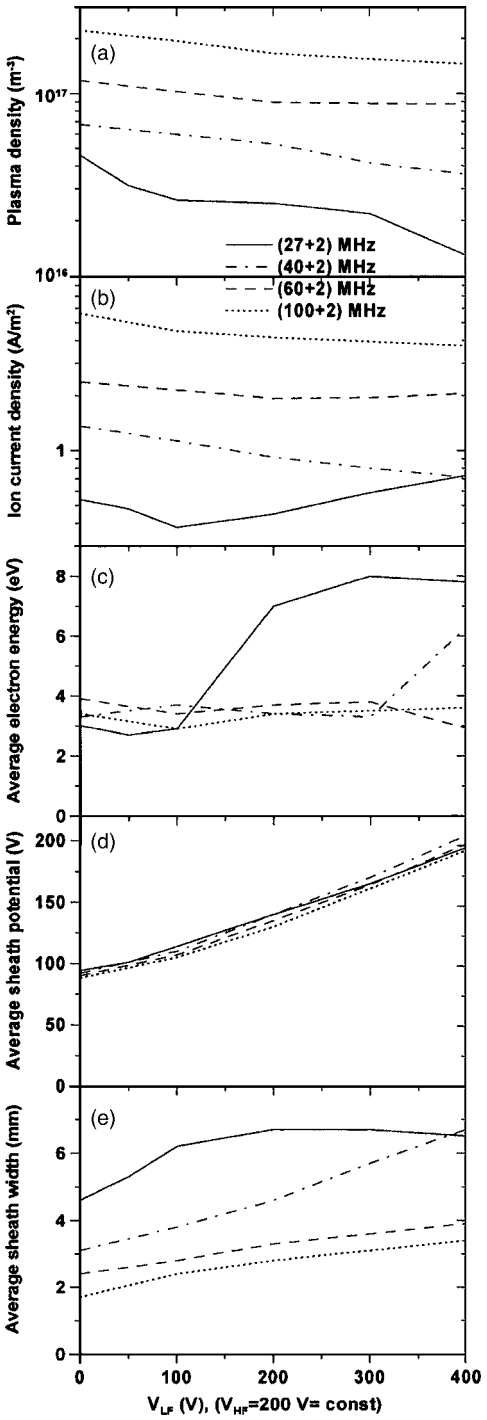

FIG. 2. Calculated plasma density in the discharge center (a), ion current density at the powered electrode (b), electron energy in the discharge center (c), and sheath potential (d) and width (e), averaged over the LF cycle, as a function of the LF voltage amplitude, at a HF voltage amplitude of 200 V for the (27+2)-, (40+2)-, (60+2)-, and (100+2)-MHz regimes.

LF voltage was also observed in computer simulations of argon discharges in a dual frequency reactor.[11,12] As it is shown below the sheath width increases with the increase of the LF voltage. The expansion of the sheath width leads to a decrease of the sheath capacitance, and therefore the discharge current decreases with increasing LF voltage. The decrease in the discharge current causes decrease in the ionization rate and consequently in the plasma density.

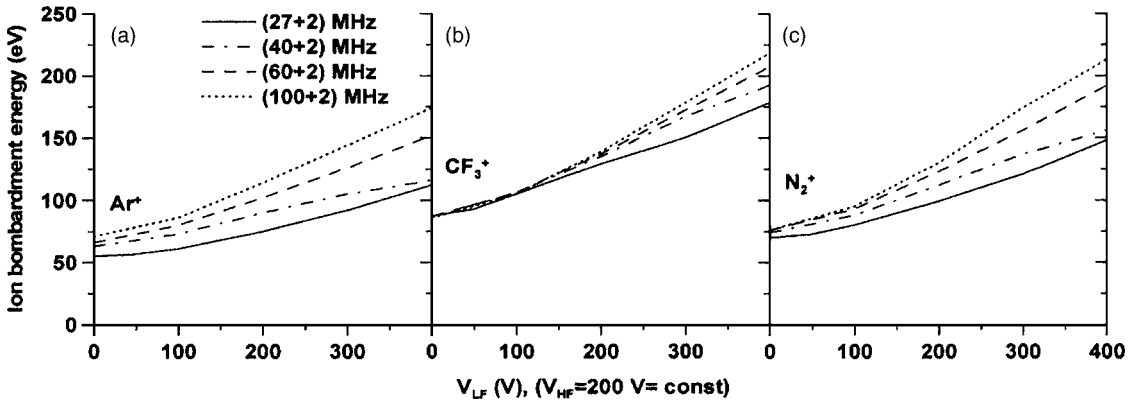

FIG. 3. Calculated Ar^+ (a), CF_3^+ (b), and N_2^+ (c) average bombardment energy as a function of the LF voltage amplitude. The operating conditions are the same as in Fig. 2.

The ion current density exhibits a similar behavior as the plasma density, with an exception for the case of (27 +2) MHz [Fig. 2(b)]. For this case the ion current density shows a minimum at a LF voltage of 100 V and because of that, we made an additional simulation at 50 V. It is observed that the ion current decreases by varying the LF voltage from 0 to 100 V and it increases with further increase of the LF voltage, i.e., the ion loss increases. On the other hand, the electron energy also increases abruptly after 100 V [Fig. 2(c)] and consequently the ionization rate, i.e., the ion production increases. The net effect of these processes is, however, a drop in the plasma density. The average electron energy and the ion current show little dependence on the LF voltage for the (60+2)- and (100+2)-MHz cases. Hence, in first instance, we would conclude that the frequency ratio should be high enough to achieve decoupling of the ion flux and energy. However, further simulations at a HF of 27 MHz and at different LF and applied voltages show that the frequency ratio is not the parameter defining the decoupling. These simulations are presented below in a separate section, where the abrupt change in the plasma behavior at a ratio V_{LF}/V_{HF} of 1 and above, when the applied HF is 27 MHz, is discussed.

A rise in the LF voltage leads to an increase of the sheath potential and to an expansion of the sheath [Figs. 2(d) and 2(e)]. A similar behavior of the sheath width was observed experimentally[4] and numerically.[11,12] On the other hand, an increase of the applied HF contracts the sheath, as it is also found in single frequency reactors,[24–26] so that in the (60 +2)- and (100+2)-MHz cases the sheath width increases more slowly than in the (27+2)- and (40+2)-MHz regimes.

Figure 3 presents the average bombardment energy of the Ar^+ (a), CF_3^+ (b), and N_2^+ (c) ions. The operating conditions are the same as in Fig. 2. The ion energy increases with LF voltage because the sheath potential increases [Fig. 2(d)]. Since the CF_3^+ ion does not experience charge exchange (see Ref. 8 for details about ion-neutral collisions), and therefore retains its energy, its average energy at the electrodes is higher, in comparison with the other two ions for the same operating conditions.

Concerning the influence of the HF, it appears from Fig. 2 that the plasma density and ion current increase, and the sheath width decreases with HF, for the same LF voltage. The electron energy is between 3 and 4 eV for all frequency conditions for a LF voltage up to 100 V, but only for the (60+2)- and (100+2)-MHz cases, it remains at similar values for higher LF voltages, i.e., it is almost not affected by the HF above 60 MHz for any investigated LF voltages. If we exclude the (27+2)-MHz case, the average sheath potential decreases very slightly with the primary frequency for the same applied LF voltage [Fig. 2(d)]. The average ion energy (Fig. 3) increases with HF because the sheath width decreases, and consequently the ions experience fewer charge exchange and elastic collisions with neutrals on their way to the electrodes, and therefore they retain their energy. A similar dependence of the plasma characteristics on the driving frequency was found in single frequency reactors.[24–26]

It is impossible to present the IEDF for all simulated operating conditions due to limited space, so that we have chosen to present them at the HF and LF voltages of 200 V for the four-frequency schemes (see Fig. 4). The average sheath potential is calculated to be between 130 and 140 V, and consequently the IEDF has two peaks and the energy width is centered at this value (see above and Ref. 8) for all frequency regimes. The second peak of Ar^+ and N_2^+ IEDFs for the (27+2)-MHz case is, however, not well developed because of the frequent charge exchange and elastic collisions with neutrals (see Ref. 8). In addition, the sheath width is broadest at the (27+2)-MHz regime, which leads to more collisions in comparison with the other frequency regimes. The bimodal structure of the IEDF in the dual frequency reactors was discussed in detail elsewhere.[8] Figure 4 shows that the energy width ΔE increases with HF when all the other operating parameters are the same. According to Eq. (2) the energy width does not depend on the HF explicitly. However, it depends on the average sheath width, which decreases with increase of the primary frequency [Fig. 2(e)]. The average sheath potential and the parameter λ_2 are calculated to be almost the same for all considered frequency schemes. Consequently, the energy width increases with HF. The same behavior was observed for the other applied LF voltage amplitudes.

In our previous study it was found that highly energetic F^- ions reach the electrodes for a short time of the cathodic part of the LF cycle.[7] In the presence of low frequency and

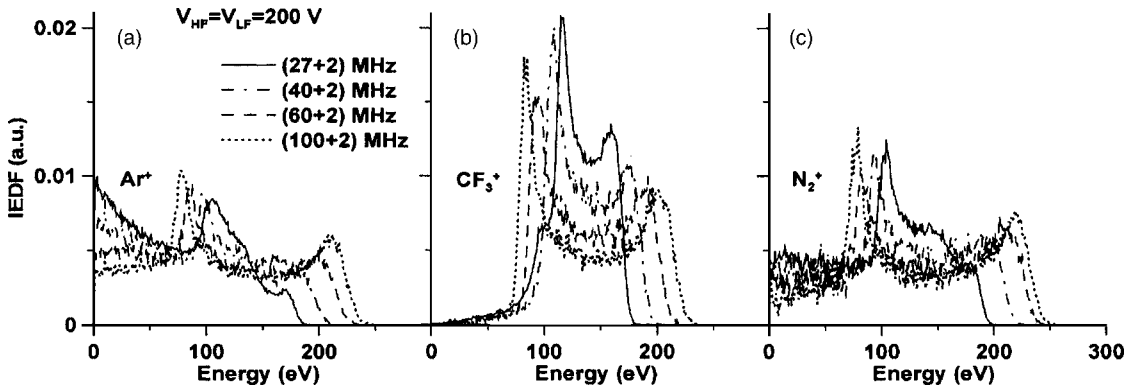

FIG. 4. Calculated Ar^+ (a), CF_3^+ (b), and N_2^+ (c) IEDF, averaged over the LF cycle, at HF and LF voltage amplitudes of 200 V for the (27+2)-, (40+2)-, (60+2)-, and (100+2)-MHz regimes.

strong electric field, the light F^- ions are no longer confined in the bulk plasma and they partially respond to the instantaneous electric field. In the present investigation it is observed that the maximum value of the F^- flux, which is calculated to be about 10^{16} m^{-2} s^{-1} for all the frequency regimes, does not increase considerably with increasing the LF voltage. Indeed, since the electric field in the sheath becomes stronger more F^- ions acquire high energy so that more ions can reach the electrodes. On the other hand, the plasma density decreases considerably for the (27+2)-MHz regime and stays more or less the same for the other frequency regimes when the LF voltage increases. Therefore, the maximum value of the F^- flux does not change with increase of the LF voltage amplitude. However, the F^- ions reach the electrodes for a longer time of the LF cycle when the LF voltage increases, and consequently the time-averaged flux increases. The incident negative ion flux on the wafer reduces the local charging, and hence it would be more useful to present the ratio of the F^- flux to the positive ion flux at the electrodes than to present only the negative ion flux. Figure 5 shows the ratio of the F^- flux to the positive ion flux, both averaged over the LF cycle, as a function of the LF voltage for the different frequency regimes. The operating conditions are the same as in Fig. 2. The ratio increases with LF voltage, except for the (27+2)-MHz regime when the LF voltage increases from 300 to 400 V. This is because the positive ion flux also increases with the LF voltage. The ratio decreases with increasing HF because the time-averaged positive flux increases while the time-averaged F^- flux decreases slightly with the HF. It is found that the negative ion flux is 0 when the LF voltage is 0, i.e., in single frequency reactors, for all investigated HFs. For the (60+2)- and (100+2)-MHz cases, the F^- flux is close to 0 even when a LF voltage of 100 V is applied [Fig. 5].

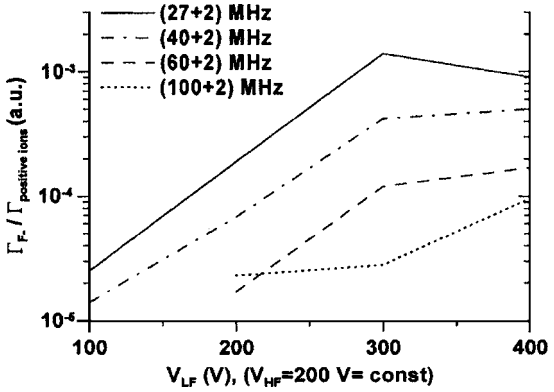

FIG. 5. Calculated ratio of F^- flux to positive ion flux at the electrodes, averaged over the LF cycle, as a function of the LF voltage amplitude. The operating conditions are the same as in Fig. 2.

B. From HF to VHF, varying the HF voltage amplitude, and keeping the LF voltage amplitude constant

Figure 6 presents the simulation results, averaged over one or two LF cycles, for the plasma density in the discharge center (a), the ion current density at the powered electrode (b), the electron energy in the discharge center (c), and the sheath potential (d)and width (e), as a function of the HF voltage amplitude. The operating conditions are the following: the HF is chosen to be 27, 40, 60, or 100 MHz and the LF is 2 MHz; the HF voltage amplitude is 100, 200, 250, 300, or 400 V and the LF voltage amplitude is kept at 200 V. Simulations for (100+2) MHz with a HF voltage above 250 V could not be performed, because the plasma density increases so much that the bulk plasma expands in the reactor volume.

The plasma density increases with HF voltage for all investigated HFs, with an exception for (27+2) MHz. In the latter case, it varies slightly from 2.4×10^{16} to 2.8×10^{16} m^{-3} when the HF voltage increases from 100 to 300 V and then it goes up to 4×10^{16} m^{-3} at a HF voltage of 400 V. The ion current shows a similar behavior as the plasma density [Fig. 6(b)]. At the same time the average electron energy decreases from 8 to 3 eV with increasing HF voltage [Fig. 6(c)] and it should therefore be expected that the ionization rate would drop, which means that the plasma density would decrease because the ion loss also increases to some extent. However, the average electron energy is not always a good characteristic of the electron energy because the EEDF $F_e(\varepsilon)$ is usually non-Maxwellian. Therefore, we present the electron energy probability function (EEPF) $f_e(\varepsilon)=F_e(\varepsilon)\varepsilon^{-1/2}$ and the ionization rate (sum of all ionization rates of electrons with Ar, CF_4 and N_2) for the (27+2)-MHz case at different HF voltages, in Figs. 7(a) and 7(b), respectively. The number of low-energy electrons increases a hundred times with HF voltage while the number

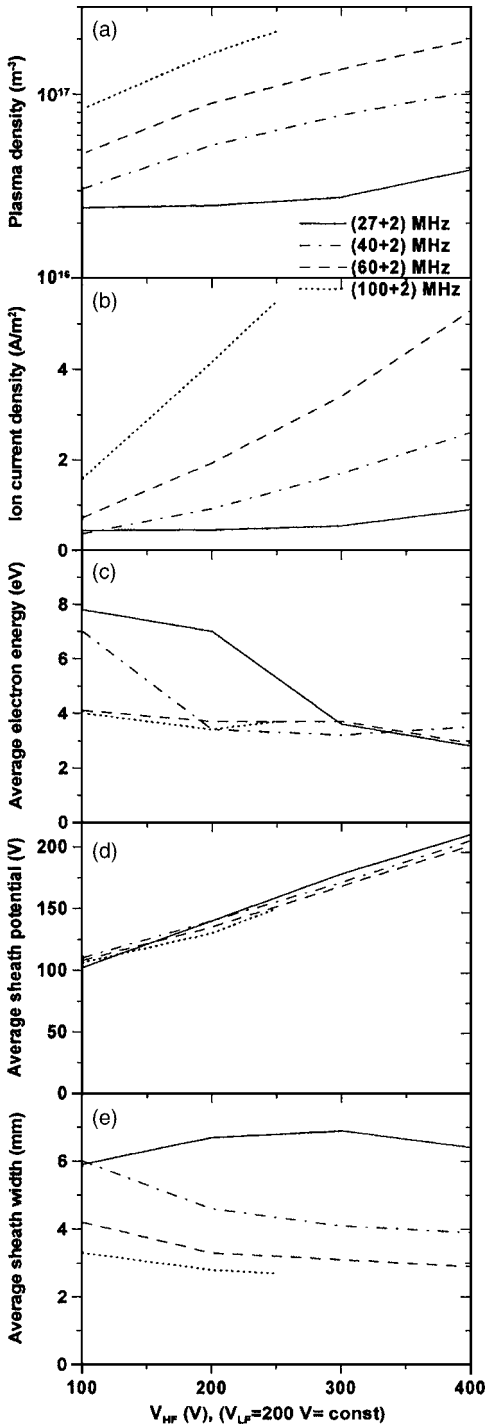

FIG. 6. Calculated plasma density in the discharge center (a), ion current density at the powered electrode (b), electron energy in the discharge center (c), and sheath potential (d) and width (e), averaged over the LF cycle, as a function of the HF voltage amplitude at a LF voltage of 200 V for the (27+2)-, (40+2)-, (60+2)-, and (100+2)-MHz regimes.

of high-energy electrons responsible for ionization increases about ten times. This explains the drop of the average electron energy [Fig. 6(c)] and the simultaneous increase of the ionization rate [Fig. 7(b)]. The peaks in the ionization rate shift with the HF voltage because of the electron density profile. Discussion follows in Sec. IV, which is focused on the influence of the LF source at a HF of 27 MHz.

For the other frequency regimes, the plasma density increases more clearly and it scales linearly with the HF voltage amplitude, which is the same voltage scale law as in single frequency reactors. [13,27] The ion current also increases with HF voltage, and as it will be shown below, it scales as $j \sim V_{HF}^{3/2}$ (see Sec. III C). Further, the electron energy is almost not affected by the HF voltage for the (60+2)- and (100+2)-MHz regimes [Fig. 6(c)]. For (40+2) MHz it decreases from 7 to 3.5 eV when the HF voltage increases from 100 to 200 V and then it stays more or less the same with further rise of the HF voltage. The electron energy in conventional cc reactors was found to be essentially independent of the applied voltage.[27] Consequently, the secondary voltage source has no influence on the plasma density, ion flux, and electron energy, except for the (27+2)-MHz case and to some extent for (40+2) MHz. In the Sec. III C we consider in detail the (60+2)-MHz regime, to show that the plasma density and ion flux can be controlled independently by the HF voltage source.

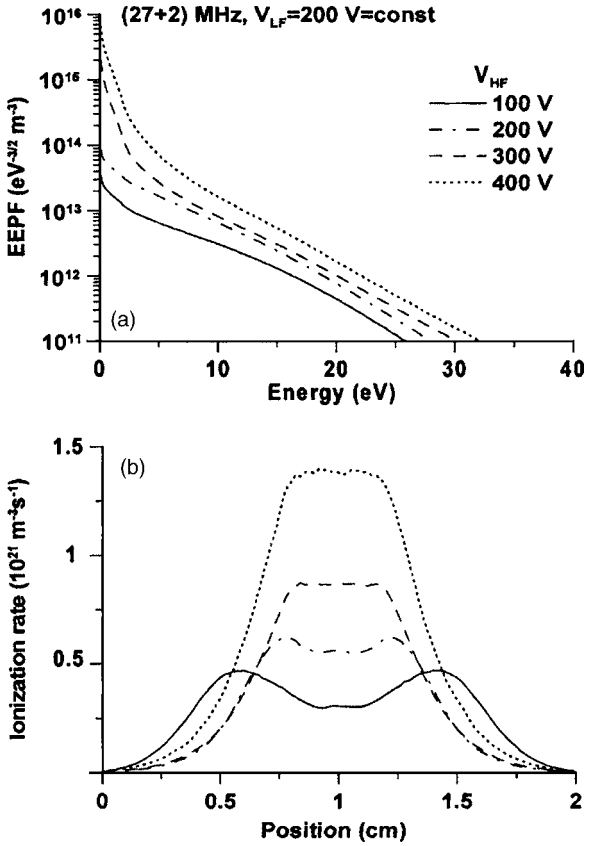

FIG. 7. Calculated EEPF (a) and electron impact ionization rates (b), averaged over the LF cycle, at a LF voltage of 200 V and different HF voltages for the (27+2)-MHz regime.

The sheath potential increases linearly with the applied HF voltage amplitude [Fig. 6(d)]. The sheath width increases slightly for (27+2) MHz and it decreases somewhat for the other regimes [Fig. 6(e)].

Figure 8 presents the average bombardment energy of the Ar^+ (a), CF_3^+ (b) and N_2^+ (c) ions, as a function of the HF voltage amplitude. The operation conditions are the same as in Fig. 6. The ion energy increases with HF voltage because the sheath potential increases [Fig. 6(d)].

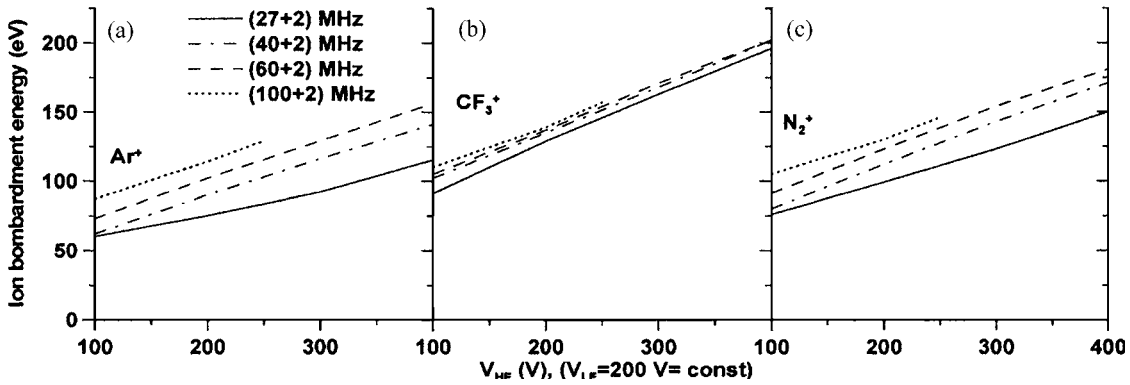

FIG. 8. Calculated Ar^+ (a), CF_3^+ (b), and N_2^+ (c) average bombardment energy as a function of the LF voltage amplitude. The operating conditions are the same as in Fig. 6.

The influence of the applied HF on the plasma characteristics is the same as in the previous section, where the HF voltage is kept constant and the LF voltage is varying (see above).

C. Independence of the plasma density, ion current density, and electron energy from the LF voltage source at (60+2) MHz

As it can be seen from the simulation results discussed above, the LF voltage has significant effect on the plasma characteristics when the HF is 27 MHz. For (40+2) MHz the dependence on the LF voltage is strong only when the LF voltage amplitude is twice as high as the HF voltage amplitude, i.e., when V_{LF} is 400 or 200 V and V_{HF} is 200 or 100 V (see Figs. 2 and 6, respectively). For the (60+2)- and (100 +2)-MHz regimes, the plasma density, ion current density, and electron energy are nearly independent from the LF voltage when the HF voltage is kept constant, and when the LF voltage is kept constant they scale with the HF voltage similar to that in single frequency reactors. In this section, we consider the simulations performed for the (60+2)-MHz regime and present additional simulation results in a single frequency reactor at a driving frequency of 60 MHz and applied voltage amplitudes of 100, 200, 300, or 400 V. Figure 9 shows the simulation results, averaged over one LF cycle, for the plasma density in the discharge center (a), the ion current density at the powered electrode (b), the electron energy in the discharge center (c), the sheath potential (left y axis) and width (right y axis) (d), and the ion energy at the driven electrode (e). The solid lines denote the results as a function of the LF voltage when the HF voltage is kept constant at 200 V. The dashed lines represent the calculations as a function of the HF voltage keeping the LF voltage constant at 200 V. Finally, the dash-dotted lines illustrate the results for a single frequency reactor of 60 MHz, as a function of the driving voltage, which is noted as V_{HF}.

The plasma density slightly decreases from 10^{17} to 9×10^{16} m^{-3} when the LF voltage increases from 100 to 400 V and the HF voltage is kept at 200 V (solid line). The ion current density is also nearly independent from the LF voltage and its value is about 2 A/m^2. The average electron energy in the bulk varies between 3 and 4 eV. It can be seen that the LF voltage does not affect the EEPF and ionization rate [Figs. 10(a) and 10(b), respectively].

For the opposite operating condition, i.e., when the HF voltage is varying and the LF voltage is kept constant at 200 V (dashed line) it is found that the plasma density scales linearly with the HF voltage V_{HF} [Fig. 9(a), dashed line]. It increases from 5×10^{16} to 2×10^{17} m^{-3}. The dotted line presents the voltage scaling law: plasma density $(n)\sim V_{HF}$. The same scaling law was observed in single frequency reactors.[13,27] Consequently, the plasma density shows the same dependence on the driving frequency, as if the second voltage source was not connected. However, the values of the plasma density are lower in comparison with the single frequency regime at the same driving voltage amplitudes [compare the dashed and dash-dotted line in Fig. 9(a)]. It was already observed that introducing the second voltage source decreases the plasma density for any of the investigated frequency schemes [Fig. 2(a)].

The ion current density j increases with HF voltage from 0.7 to 5.3 A/m^2 [Fig. 9(b), dashed line]. It is found to scale as $j\sim V_{HF}^{3/2}$ [see the dotted line in Fig. 9(b)]. The simulation results in single frequency regime show that the ion current density scales as $j\sim V_{HF}^{1.45}$ [Fig. 9(b), dash-dotted line]. Therefore, like the plasma density, the ion current density shows the same dependence on the driving frequency as if the second voltage source was not connected, but its values are somewhat lower than that in the single frequency reactor for the same HF voltage amplitude.

The electron energy in the bulk varies between 3 and 4 eV. It can be seen that the slope of the EEPF is almost the same for all investigated HF voltage amplitudes [Fig. 11(a)], and the distribution is more or less Maxwellian so that the average electron energy does not change considerably. The number of high-energy electrons increases with HF voltage and consequently the ionization rate also increases [Fig. 11(b)]. When only one frequency is applied, the behavior of the average electron energy [Fig. 9(c) dash-dotted line] as well as the EEPF and ionization rate are very similar. For that reason we do not present the calculated EEPF and the ionization rates in single frequency regime here.

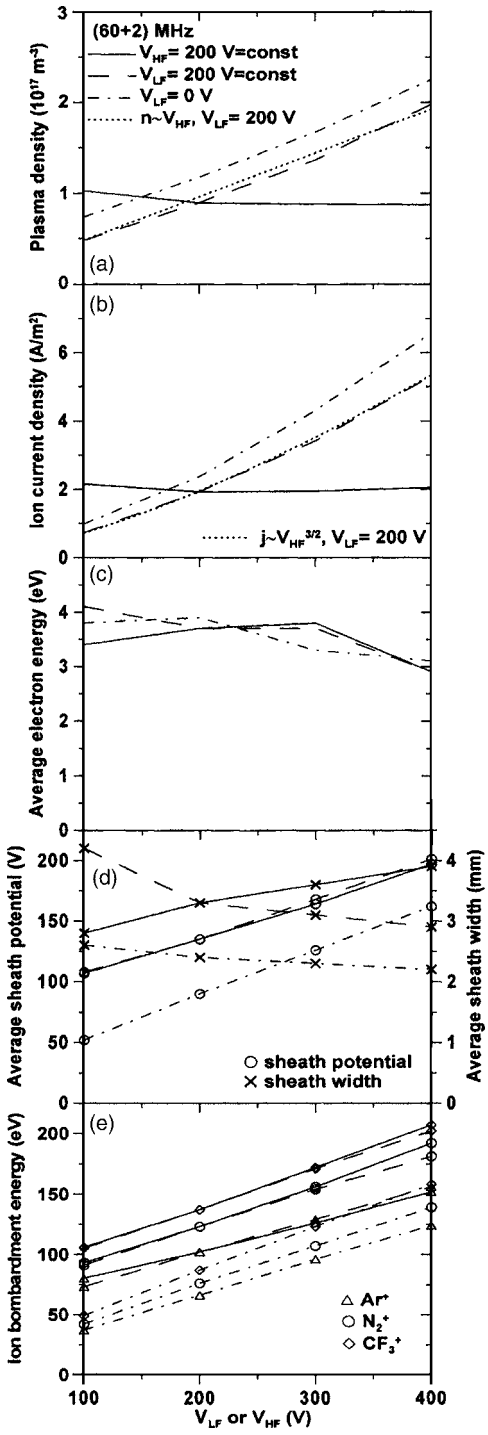

FIG. 9. Calculated plasma density in the discharge center (a), ion current density at the powered electrode (b), electron energy in the discharge center (c), sheath potential (left y axis) and width (right y axis) (d), and ion bombardment energy (e), averaged over the LF cycle, as a function of the LF voltage amplitude (solid lines) or HF voltage amplitude (dashed lines) for the (60+2)-MHz regime. The results for a single frequency reactor at 60 MHz are shown as a function of the driving voltage (dash-dotted lines). Finally, the dotted lines present the scaling law of the plasma density $n \sim V_{\mathrm{HF}}$ (a) and of the ion current density $j \sim V_{\mathrm{HF}}^{3/2}$ (b) with the applied HF voltage amplitude at a LF voltage of 200 V.

D. Dependence of the sheath potential and width, and the ion energy on the HF and LF voltage sources

Below we discuss the simulation results of the sheath potential and width, and the ion energy for the (60+2)-

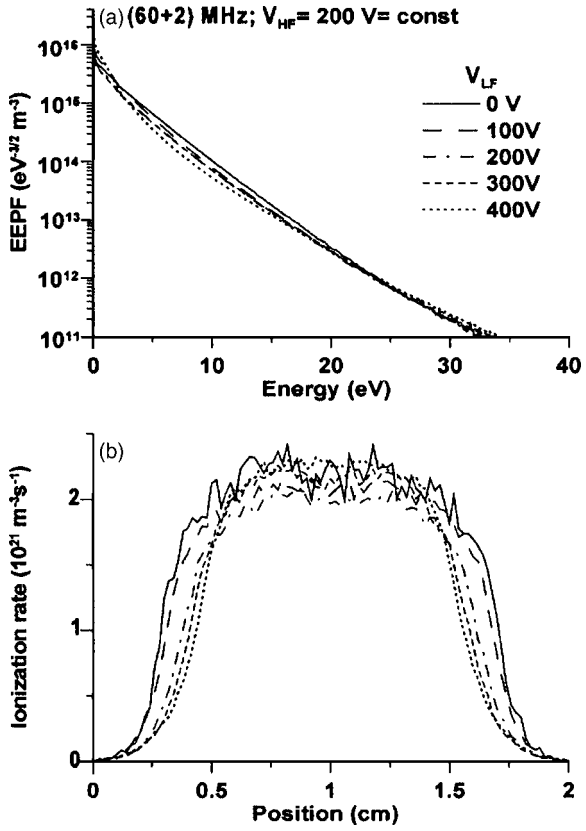

FIG. 10. Calculated EEPF (a) and electron impact ionization rates (b), averaged over the LF cycle, at a HF voltage of 200 V and different LF voltages for the (60+2)-MHz regime.

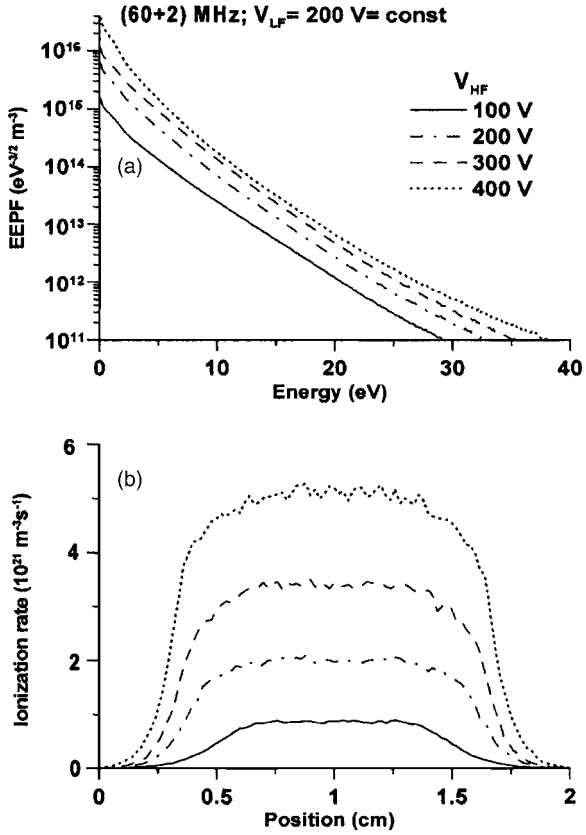

FIG. 11. Calculated EEPF (a) and electron impact ionization rates (b), averaged over the LF cycle, at a LF voltage of 200 V and different HF voltages for the (60+2)-MHz regime.

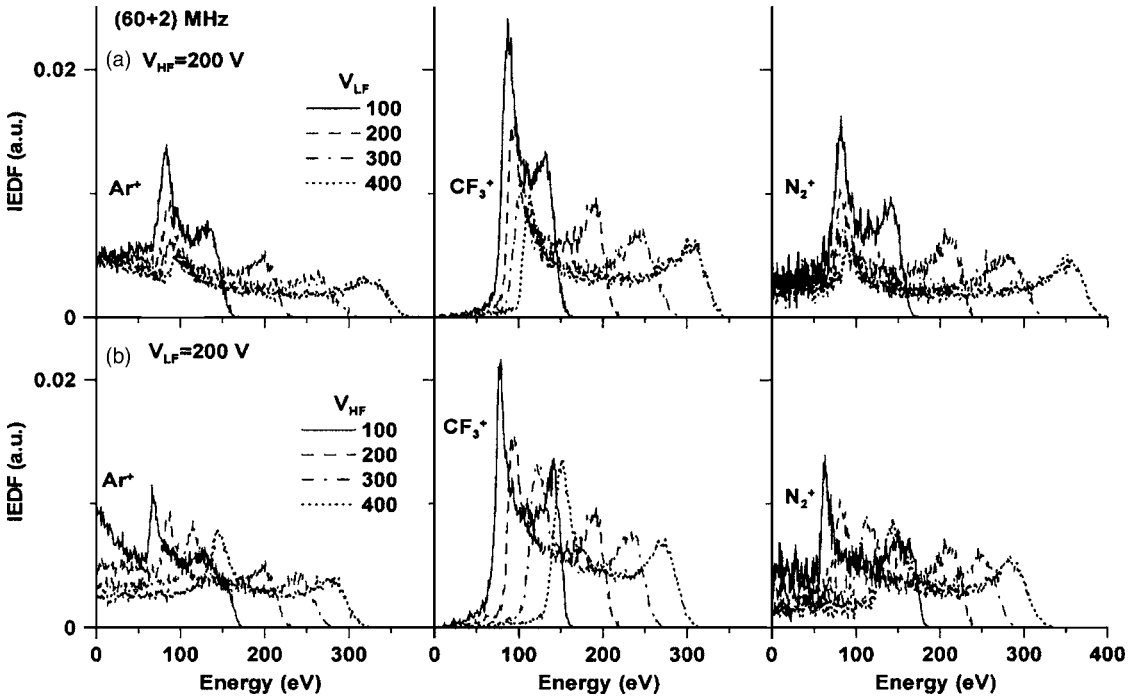

FIG. 12. Calculated Ar^+, CF_3^+, and N_2^+ IEDF, averaged over the LF cycle, for the (60+2)-MHz regime at a HF voltage amplitude of 200 V and different LF voltage amplitudes (a), and at a LF voltage amplitude of 200 V and different HF voltage amplitudes (b).

MHz case. However, it should be noted that these characteristics exhibit a similar behavior in the other investigated frequency regimes.

The sheath potential increases linearly with the applied voltage and consequently with the LF or HF voltage amplitude [Fig. 9(d), left y axis, solid and dashed lines, respectively, and see Eq. (1)].

The sheath expands from 2.8 to 3.9 mm [Fig. 9(d), right y axis, solid line] with the increase of LF voltage, and it contracts from 4.4 to 2.9 mm with increase of the HF voltage in the dual frequency regime [Fig. 9(d), right y axis, dashed line], but it is wider in comparison with the single frequency case for the same HF voltage (compare with dash-dotted line). The sheath width is essentially independent from the applied voltage in the single frequency case [Fig. 9(d), right y axis, dash-dotted line]. Other authors also observed that the applied voltage did not influence the sheath width in a single frequency reactor.[27,28]

The average ion bombardment energy [Fig. 9(e)] increases with both the LF or HF voltage amplitude, because the sheath potential increases with the applied voltage [see Fig. 9(d)]. Figure 12 presents the IEDFs of the three considered positive ions in the (60+2)-MHz regime at LF voltages of 100, 200, 300, and 400 V and a HF voltage of 200 V (a); and at HF voltages of 100, 200, 300, and 400 V and a LF voltage of 200 V (b). The IEDF is broader when the LF or HF voltage increases, while keeping the other voltage constant. It should be noted that the IEDF depends on the voltages in the same way for all frequency regimes. Hence, we present only the results here for (60+2) MHz.

The average ion energy is calculated to have similar values when the sum of the LF and HF voltages is the same [cf. solid and dashed lines in Fig. 9(e)] because the average ion energy follows the average sheath potential $\bar{V}_s$, in spite of the fact that the IEDF appears to be broader when the LF voltage amplitude is larger [for example, cf. the dotted lines in Figs. 12(a) and 12(b)]. The energy width is centered at $e\bar{V}_s$ (see above and Ref. 8) and when the IEDF is wider the first maximum appears at lower energy if the $\bar{V}_s$ is the same. Consequently, although the maximum energy is higher when the LF voltage is larger, the average ion energy has similar values in the case of equal sum of HF and LF voltage amplitudes like the average sheath potential has similar values (see Fig. 9(d), left y axis, solid and dashed lines).

Let us compare the Ar^+ IEDF for HF and LF voltage amplitudes of 200 and 400 V, and 400 and 200 V, respectively, so that their sum is 600 V in both cases (Fig. 12, dotted lines). The energy width is about 230 eV at LF voltage of 400 V and HF voltage of 200 V and only 135 eV at LF voltage of 200 V and HF voltage of 400 V. The sheath width is calculated to be 3.9 and 2.9 mm, respectively, for the two considered cases [Fig. 9(d), right y axis]. Because the average sheath potential and the LF are the same, from Eq. (2), one should expect that the IEDF is broader at a LF voltage of 200 V and a HF voltage of 400 V since the sheath width is smaller. In fact, the opposite is observed. The reason can be found in the different sheath potential form as a function of the phase in the LF cycle. Numerically, this information is contained in the parameter λ_2 (see Ref. 8 for details about the calculation of λ_2), which is calculated to be 0.72 and 0.3 at LF voltage amplitudes of 400 and 200 V, respectively. Figure 13 presents the sheath potential in different phases of the LF cycle, when the HF and LF voltage amplitudes are 200 and 400 V (a), and 400 and 200 V (b), respectively. The ion transit time is calculated to be much longer

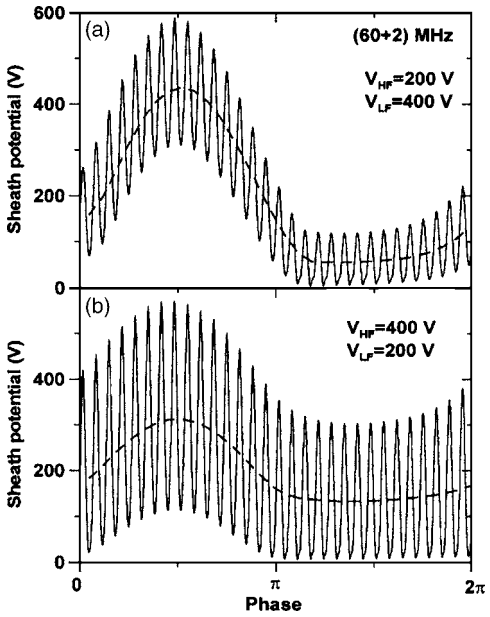

FIG. 13. Calculated sheath potential as a function of the phase in the LF cycle, for the (60+2)-MHz regime at HF and LF voltage amplitudes of 200 and 400 V (a), and 400 and 200 V, respectively (b). The dashed lines present the average HF sheath potential as a function of the phase in the LF cycle.

than the HF period and comparable to the LF period, and therefore the ions respond to the average HF sheath potential, which is a function of the LF (see the dashed lines in Fig. 13).[8] The averaged minimum and maximum of the sheath potentials are 55 and 430 V [Fig. 13(a)], and 130 and 310 V [Fig. 13(b)], respectively. The two outstanding peaks in the IEDF profiles (Fig. 12) correspond to the averaged minimum and maximum sheath potentials.[8] This explains the broader energy distribution when the LF voltage amplitude is larger than the HF voltage, in comparison with the opposite case. This observation is valid for all investigated frequency regimes. Consequently, the ion energy depends on both voltage sources and cannot be controlled independently by the LF source. However, the IEDF is broader by increasing the LF voltage and keeping the sum of the LF and HF voltages constant.

E. Dependence of the plasma characteristics on the LF voltage source at (27+2)- and (27+1)-MHz regimes

As it is discussed above, the LF source has critical influence on the plasma density, ion flux, and electron energy at (27+2) MHz [Figs. 2(a)–2(c)]. Further simulations were performed at the (27+2)- and (27+1)-MHz regimes in order to explain the nonlinear dependence of the plasma behavior on the LF voltage source. Figure 14 presents the simulation results averaged over one or two LF cycles, for the plasma density in the discharge center (a), the ion current density at the powered electrode (b), the electron energy in the discharge center (c), the sheath potential (left y axis) and width (right y axis) (d), and the ion energy at the driven electrode (e). The solid and dashed lines represent the calculation results for the (27+2)- and (27+1)-MHz regimes, respectively,

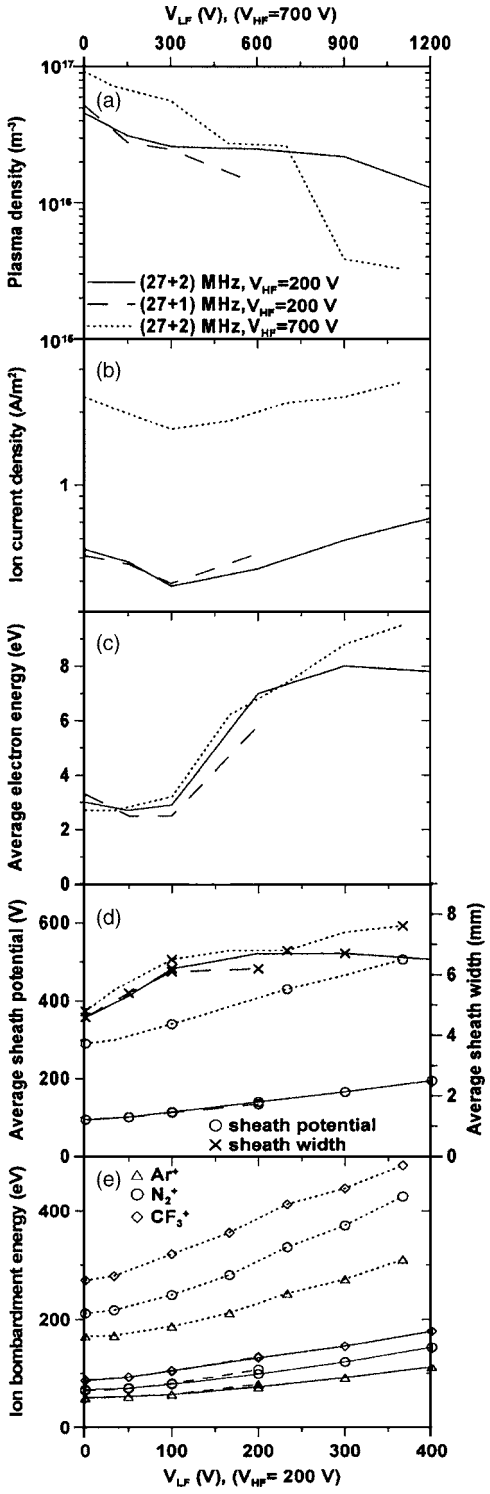

FIG. 14. Calculated plasma density in the discharge center (a), ion current density at the powered electrode (b), electron energy in the discharge center (c), sheath potential (left y axis) and width (right y axis) (d), and ion bombardment energy (e), averaged over the LF cycle, as a function of the LF voltage amplitude, at a HF voltage of 200 V, for (27+2) (solid lines, bottom x axis) and (27+1) MHz (dashed lines, bottom x axis), as well as at a HF voltage of 700 V for (27+2) MHz (dotted lines, top x axis).

at a HF voltage of 200 V and LF voltages of 0, 50, 100, 200, 300, and 400 V (bottom x axis). In the same figure, the results are also shown for the (27+2)-MHz case at a HF voltage of 700 V and LF voltages of 0, 100, 300, 500, 700, 900, and 1100 V (dotted line and top x axis). The simulations for

(27+1) MHz, when the LF voltage is higher than 200 V, could not be performed because the two sheaths expand and become comparable with the electrode gap, so that the plasma cannot be sustained.

The same trend is observed in the effect of the LF voltage on the plasma behavior in the three investigated cases. The plasma density considerably decreases with the LF voltage [Fig. 14(a)]. The ion current density has a minimum at LF to HF voltage ratio V_{LF}/V_{HF} of about 0.5, i.e., when the LF voltage is 100 or 300 V and the HF voltage is 200 or 700 V, respectively. Further, the ion current density increases with the LF voltage amplitude [Fig. 14(b)]. The electron energy has more or less the same values for V_{LF}/V_{HF} up to 0.5 and then it increases abruptly [Fig. 14(c)].

We suppose that the reason for the observed nonlinear plasma characteristics is the transition from electropositive to electronegative plasma behavior when the ratio V_{LF}/V_{HF} is 1 and higher (e.g., at a HF voltage of 200 V and LF voltages of 200, 300, and 400 V in Figs. 2 and 14, and at HF voltages of 100 and 200 V, and a LF voltage of 200 V, for the (27+2) regime, presented in Fig. 6). This transition was noticed in the Ar/CF_4 discharge when the CF_4 concentration was increased.[14] At low concentration of CF_4 (10%) the discharge exhibits more electropositive features, such as the electric field in the center is close to 0, and consequently the electron energy is about 3 eV. The electron density has a flat profile. However, the main negative species are the F^- and CF_3^- ions.[14] The same features are observed in the presented dual frequency reactor at a ratio V_{LF}/V_{HF} below 1.

On the other hand, at high concentration (90%) of CF_4 the discharge is definitely electronegative and the double layer of the electric field and the electron density maxima at the bulk-sheath interface are well established. The substantial bulk electric field leads to average electron energy in the bulk of 6 eV and higher. The electronegativity ($=n_n/n_e$, where n_n and n_e denote the negative ion and electron densities, respectively) increases with the concentration of CF_4.[14] This behavior is also observed in the dual frequency reactor at a ratio V_{LF}/V_{HF} of 1 and higher, although the CF_4 concentration is only 10%. For example, for the (27+2)-MHz regime the electronegativity increases from 6 to 35 when the LF voltage increases from 100 to 400 V at a HF voltage of 200 V, and it decreases from 60 to 3 when the HF voltage increases from 100 to 400 V at a LF voltage of 200 V. At a ratio V_{LF}/V_{HF} of 1 and higher, the electric-field distribution has a profile similar to that presented in Ref. 7 for the dual frequency reactor and in Ref. 14 at 90% concentration of CF_4, i.e., the double layer structure appears and the electric field in the bulk is substantial (up to a several thousands of V/m). The strong electric field in the bulk explains the abrupt increase in the electron energy from 3 to 7 eV and higher in Figs. 2(c) and 14(c), as well as the abrupt decrease in the electron energy at a HF of 300 V for the (27+2)-MHz regime in Fig. 6(c). When the ratio V_{LF}/V_{HF} is below 1 the electric field in the center is close to 0 and the profile is similar to that in electropositive discharges (see Ref. 14).

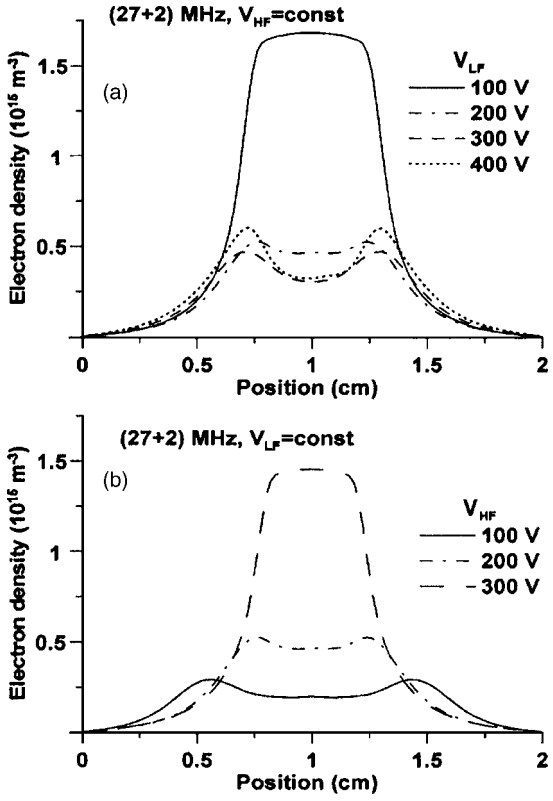

FIG. 15. Calculated electron density distribution, averaged over the LF cycle, at a HF voltage of 200 V and a LF voltage of 100, 200, 300, and 400 V (a), and at a LF voltage of 200 V and a HF voltage of 100, 200, and 300 (b) for the (27+2)-MHz regime.

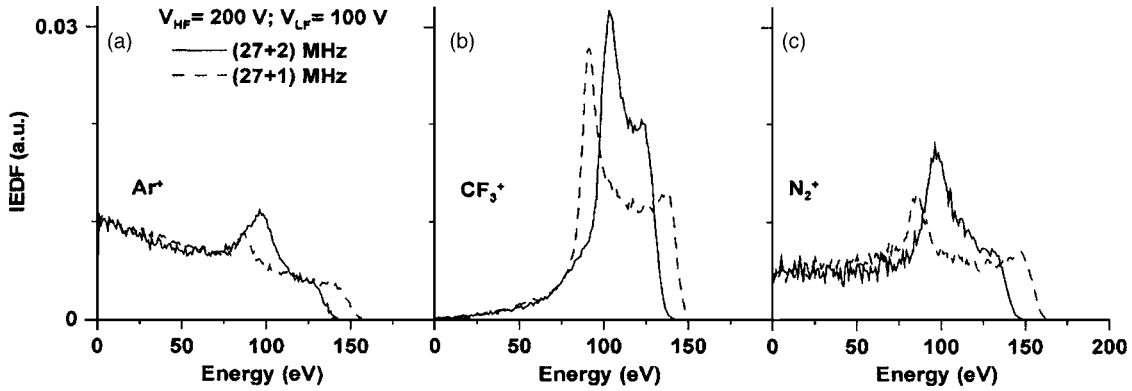

FIG. 16. Calculated Ar^+ (a), CF_3^+ (b), and N_2^+ (c) IEDF, averaged over the LF cycle, at HF and LF voltage amplitudes of 200 and 100 V, respectively, for (27+2) (solid lines) and (27+1) MHz (dashed lines).

TABLE I. The calculated HF and LF powers in W for the (27+2)-, (40+2)-, (60+2)-, (100+2)-, and (27+1)-MHz regimes when the HF voltage is kept constant at 200 V and the LF voltage is varying.

	(27+2) MHz		(40+2)MHz		(60+2) MHz		(100+2) MHz		(27+1) MHz	
V_{LF} (V)	P_{HF} (W)	P_{LF} (W)	P_{HF}	P_{LF}	P_{HF}	P_{LF}	P_{HF}	P_{LF}	P_{HF}	P_{LF}
0	5	0	13	0	25	0	61	0	5	0
50	4	1	12	1	⋯	⋯	⋯	⋯	4	1
100	3	1	10	3	20	5	48	10	4	1
200	3	2	8	5	17	10	41	20	4	3
300	4	5	6	6	16	16	37	32	⋯	⋯
400	5	8	5	8	15	23	34	43	⋯	⋯

Because of the limited space, in Fig. 15 we present only the electron density distribution, averaged over the LF cycle, at a HF voltage of 200 V and LF voltages of 100, 200, 300, and 400 V (a), and at a LF voltage of 200 V and HF voltages of 100, 200, and 300 (b). In order to make the plots clear we do not present the electron density distributions at LF voltages of 0 and 50 V and a HF voltage of 200 V, and at a HF voltage of 400 V and a LF voltage of 200 V. For these cases the profile is flat and the electron densities in the bulk are 3.1×10^{15}, 3×10^{15}, and 4.5×10^{15}, respectively. The transition from electropositive to electronegative behavior is observed with increase of the V_{LF}/V_{HF} ratio. The profile of the average electron density [Fig. 15(b)] and the electron energy distribution [see Fig. 7(a)] explains the dependence of the ionization rate profile presented in Fig. 7(b) on the HF voltage. Consequently, at a HF of 27 MHz, the plasma production depends not only on the HF source but also on the LF source when the voltage ratio V_{LF}/V_{HF} is close to 1 or higher, which corresponds to the close values of the calculated power of the two sources or when the LF power exceeds the HF power (see the Appendix).

Although the (27+1) and (60+2) regimes have a similar HF/LF ratio, it is observed that the LF voltage source has substantial influence on the ion current density and plasma density at a HF of 27 MHz and the decoupling is possible only at higher primary frequencies. Therefore, independent control of plasma density and ion current is determined by the primary frequency and not by the frequency ratio, which was also experimentally observed.[4]

The sheath voltage and width increase with the LF voltage because the applied voltage increases [Fig. 14(d)]. The ion bombardment energy also increases with the LF voltage amplitude. It has very similar values for the (27+1)- and (27+2)-MHz cases when the HF voltage is kept constant at 200 V [Fig. 14(e), solid and dashed lines]. However, the IEDF is broader at the LF of 1 MHz when all the other operating conditions are the same (Fig. 16). As it can be deduced from Eq. (2) the energy width is indeed inversely proportional to the LF. A more detailed discussion about the dependence of the energy width on the LF in a dual frequency reactor can be found in Ref. 8.

IV. SUMMARY

A detailed numerical investigation by means of the PIC/MC method was made to study the influence of the reactor parameters on the plasma characteristics in $Ar/CF_4/N_2$ plasmas in a dual frequency reactor. The calculated plasma density and electron energy in the discharge center, ion flux and energy onto the electrodes, the sheath potential and width, the EEPF and IEDF, and ionization rates were presented as a function of the LF or HF voltage amplitude and applied LF or HF.

It is observed that the decoupling of the two sources is possible with increase of the applied HF to values of 60 MHz and higher, and it is not defined by the frequency ratio. Both voltage sources have influence on the plasma characteristics at HF of 27 MHz and to some extent at 40 MHz. At HF of 60 and 100 MHz, the plasma density and ion current density show the same dependence on the driving frequency as if the second voltage source was not connected, but their values are somewhat lower than that in the single frequency reactor for the same HF voltage amplitude. The electron energy, EEPF, and ionization rates are almost unaffected by the LF source. The sheath potential increases with the HF or LF voltage amplitude because the applied voltage increases. The sheath width slightly increases with LF voltage and slightly decreases with HF voltage, while it is not influenced by the driving voltage in the single frequency reactor.

The plasma density and ion current increase, and the sheath width decreases with HF when the other operating conditions are the same. The average sheath potential decreases very slightly with the primary frequency. The average ion energy increases with HF because the sheath width

TABLE II. The calculated HF and LF powers in W for the (27+2)-MHz regime when the HF voltage is kept constant at 700 V and the LF voltage is varying.

	(27+2) MHz	
V_{LF} (V)	P_{HF} (W)	P_{LF} (W)
0	51	0
100	45	4
300	34	12
500	31	23
700	33	40
900	31	52
1100	32	72

TABLE III. The calculated HF and LF powers in W for the (27+2)-, (40+2)-, (60+2)-, and (100+2)-MHz regimes, when the HF voltage is kept constant at 200 V and the LF voltage is varying. The calculated power in single frequency of 60 MHz is also given.

	(27+2)MHz		(40+2)MHz		(60+2)MHz		60 MHz	(100+2) MHz	
V_{HF} (V)	P_{HF} (W)	P_{LF} (W)	P_{HF}	P_{LF}	P_{HF}	P_{LF}	P	P_{HF}	P_{LF}
100	2	2	2	2	4	4	8	11	9
200	3	2	8	5	17	10	25	41	20
250	⋯	⋯	⋯	⋯	⋯	⋯	⋯	63	26
300	6	3	19	8	39	16	55	⋯	⋯
400	11	4	34	12	73	24	71	⋯	⋯

decreases. A similar dependence of the plasma characteristics on the driving frequency was found in single frequency reactors.

The average ion bombardment energy increases with HF or LF voltage amplitude when the other voltage amplitude is kept constant, because the sheath potential increases with the sum of the applied HF and LF voltages. However, the IEDF becomes broader by increasing the LF voltage and keeping the sum of the LF and HF voltages constant, i.e., the average sheath potential is the same. Finally, the ion energy distribution function is broader with the increase of HF or the decrease of LF.

In conclusion, independent control of the ion flux and energy in a voltage driven dual frequency reactor is possible by increasing the HF and varying the LF voltage when the HF voltage is kept constant. The present study covers a wide range of different applied voltages and frequencies of the dual frequency reactor so that they can be adjusted to obtain desirable plasma characteristics and therefore this study can be useful in improving control over the etching process.

ACKNOWLEDGMENTS

We would like to thank R. Gijbels for helpful discussions. This research is supported by the Federal Services for Scientific, Cultural and Technical Affairs of the Prime Minister's Office through IUAP—V.

APPENDIX

In our model, the applied voltage is the determining parameter. However, because the experimentalists might be more familiar with the applied power, the calculated power of the two sources, corresponding to the different applied voltages, is presented for all investigated frequency regimes.

Table I shows the calculated HF and LF powers in watts, for the (27+2)-, (40+2)-, (60+2)-, (100+2)-, and (27+1)-MHz regimes when the HF voltage is kept constant at 200 V and the LF voltage is varying. The LF power increases and the HF power decreases with the LF voltage. For a HF of 27 MHz the HF power decreases until it reaches comparable values with the LF power and then increases or does not change (see also Table II). Table II presents the calculated HF and LF powers in watts, for the (27+2)-MHz regime when the HF voltage is kept constant at 700 V and the LF voltage is varying.

Table III shows the calculated HF and LF powers in watts, for the (27+2)-, (40+2)-, (60+2)-, and (100+2)-MHz regimes when the LF voltage is kept constant at 200 V and the HF voltage is varying, and in the single frequency reactor at 60 MHz. The HF and LF powers increase when the HF voltage increases.

[1] H. H. Goto, H.-D. Löwe, and T. Ohmi, J. Vac. Sci. Technol. A **10**, 3048 (1992); IEEE Trans. Semicond. Manuf. **6**, 58 (1993).
[2] F. R. Myers, M. Ramaswami, and T. S. Cale, J. Electrochem. Soc. **141**, 1313 (1994).
[3] H. C. Kim and V. I. Manousiouthakis, J. Vac. Sci. Technol. A **16**, 2162 (1998).
[4] T. Kitajima, Y. Takeo, and T. Makabe, J. Vac. Sci. Technol. A **17**, 2510 (1999); T. Kitajima, Y. Takeo, Z. Lj. Petrović, and T. Makabe, Appl. Phys. Lett. **77**, 489 (2000).
[5] S. Rauf and M. J. Kushner, IEEE Trans. Plasma Sci. **27**, 1329 (1999).
[6] K. Maeshige, G. Washio, T. Yagisawa, and T. Makabe, J. Appl. Phys. **91**, 9494 (2002).
[7] V. Georgieva, A. Bogaerts, and R. Gijbels, J. Appl. Phys. **94**, 3748 (2003).
[8] V. Georgieva, A. Bogaerts, and R. Gijbels, Phys. Rev. E **69**, 026406 (2004).
[9] G. Wakayama and K. Nanbu, IEEE Trans. Plasma Sci. **31**, 638 (2003).
[10] J. K. Lee, N. Yu. Babaeva, H. C. Kim, O. V. Manuilenko, and J. W. Shon, IEEE Trans. Plasma Sci. **32**, 47 (2004).
[11] P. C. Boyle, A. R. Ellingboe, and M. M. Turner, Plasma Sources Sci. Technol. **13**, 493 (2004).
[12] P. C. Boyle, A. R. Ellingboe, and M. M. Turner, J. Phys. D **37**, 697 (2004).
[13] M. A. Lieberman and A. J. Lichtenberg, *Principles of Plasma Discharges and Materials Processing* (Wiley, New York, 1994).
[14] V. Georgieva, A. Bogaerts, and R. Gijbels, J. Appl. Phys. **93**, 2369 (2003).
[15] A. Vasenkov and M. Kushner, J. Appl. Phys. **95**, 834 (2004).
[16] S. Rauf, IEEE Trans. Plasma Sci. **31**, 471 (2003).
[17] C. K. Birdsall and A. B. Langdon, *Plasma Physics via Computer Simulation* (McGraw-Hill, New York, 1985).
[18] V. Vahedi and M. Surendra, Comput. Phys. Commun. **87**, 179 (1995).
[19] A. Okhrimovskyy, A. Bogaerts, and R. Gijbels, Phys. Rev. E **65**, 037402 (2002).
[20] E. Kawamura, C. K. Birdsall, and V. Vahedi, Plasma Sources Sci. Technol. **9**, 413 (2000).
[21] N. V. Mantzaris, A. Boudouvis, and E. Gogolides, J. Appl. Phys. **77**, 6169 (1995); E. Gogolides, M. Stathakopoulos, and A. Boudouvis, J. Phys. D **27**, 1878 (1994).
[22] J. P. Booth, G. Cunge, P. Chabert, and N. Sadeghi, J. Appl. Phys. **85**, 3097 (1999).
[23] F. Debal, J. Bretagne, M. Jumet, M. Wautelet, J. P. Dauchot, and M. Hecq, Plasma Sources Sci. Technol. **7**, 219 (1998).
[24] M. Surendra and D. B. Graves, Appl. Phys. Lett. **59**, 2091 (1991).
[25] V. Vahedi, C. K. Birdsall, M. A. Lieberman, G. DiPeso, and T. D. Rognlien, Phys. Fluids B **5**, 2719 (1993).
[26] T. Kitamura, N. Nakano, T. Makabe, and Y. Yamaguchi, Plasma Sources Sci. Technol. **2**, 40 (1993).
[27] M. Surendra and D. Graves, IEEE Trans. Plasma Sci. **19**, 144 (1991).
[28] D. Vender and R. W. Boswell, IEEE Trans. Plasma Sci. **18**, 144 (1990).